LA-UR 09-03574

# Development of Self-Interrogation Neutron Resonance Densitometry (SINRD) to Measure the $^{235}$U and $^{239}$Pu Content in a PWR 17x17 Spent Fuel Assembly

**A.M. LaFleur[1], W.S. Charlton[1], H.O. Menlove[2], and M. Swinhoe[2]**

[1]Nuclear Security Science and Policy Institute, College Station, TX 77843
[2]Los Alamos National Laboratory, Los Alamos, NM 87545
amlafleur@tamu.edu; wcharlton@tamu.edu; hmenlove@lanl.gov; swinhoe@lanl.gov;

***Abstract:***

*The use of Self-Interrogation Neutron Resonance Densitometry (SINRD) to measure the $^{235}$U and $^{239}$Pu content in a PWR spent fuel assembly was investigated via Monte Carlo N-Particle eXtended transport code (MCNPX) simulations. The sensitivity of SINRD is based on using the same fissile materials in the fission chambers as are present in the fuel because the effect of resonance absorption lines in the transmitted flux is amplified by the corresponding (n,f) reaction peaks in fission chamber. These simulations utilize the $^{244}$Cm spontaneous fission neutrons to self-interrogate the fuel pins. The amount of resonance absorption of these neutrons in the fuel can be measured using $^{235}$U and $^{239}$Pu fission chambers placed adjacent to the assembly. We used ratios of different fission chambers to reduce the sensitivity of the measurements to extraneous material present in fuel. The development of SINRD to measure the fissile content in spent fuel is of great importance to the improvement of nuclear safeguards and material accountability. Future work includes the use of this technique to measure the fissile content in FBR spent fuel and heavy metal product from reprocessing methods.*

**Keywords:** spent fuel, nuclear safeguards, fissile content, plutonium

## 1. Introduction

The development of non-destructive assay (NDA) capabilities to measure the fissile content in nuclear fuels is crucial to the implementation of effective international safeguards. The use of self-interrogation neutron resonance densitometry (SINRD) for the assay of fissile materials is a promising technique for nuclear safeguards and material accountability measurements. The neutron resonance cross-section structure is unique for each of the fissionable isotopes such as $^{235}$U, $^{233}$U, $^{239}$Pu, and $^{241}$Pu, and the resonance structure can provide a signature for the measurement of these materials of importance for safeguards and non-proliferation. The sensitivity of this technique is based on using the same fissile materials in the sample and fission chamber because the effect of resonance absorption lines in the transmitted flux is amplified by the corresponding (*n,f*) reaction peaks in the fission chamber. Thus, a $^{235}$U fission chamber has high sensitivity to the neutron resonance absorption in $^{235}$U that is in the sample, and similarly for the other fissile isotopes. The self-interrogation signature is a result of having the same fissile material in the fission chamber as in the sample [1].

In Fig. 1, the $^{239}$Pu fission cross-section is compared to the resonance absorption lines in the neutron flux after transmission through a Gd filter and 0.25-mm [curve (a)] and 2.54-mm [curve (b)] $^{239}$Pu metal sample. It is important to note that as the sample thickness increases, the self- interrogation signature decreases due to self-shielding effects occurring from saturation of the larger resonances [2].

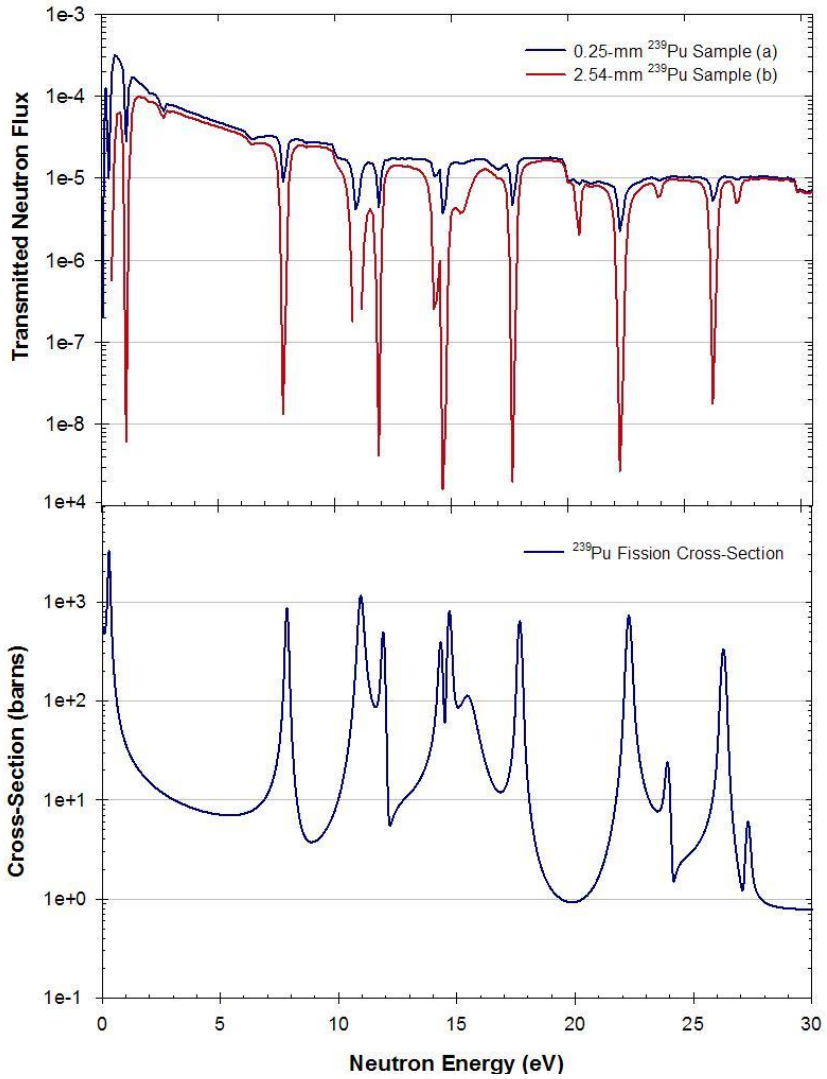


**Figure 1.** Comparison of absorption lines in the neutron flux after transmission through a 0.114-mm Gd filter and 0.25-mm [curve (a)] and 2.54-mm [curve (b)] $^{239}$Pu metal sample (upper plot) to the $^{239}$Pu fission cross-section at neutron energies ≤ 30 eV (bottom plot) [2].

The primary objective of this research is to develop and assess the sensitivity of using Self-Interrogation Neutron Resonance Densitometry (SINRD) for nuclear safeguards measurements. Recent interest in this approach was stimulated by an IAEA request related to spent fuel verification. Prior measurements [3,4] and calculations [1] have demonstrated that the SINRD method gives quantitative results for the fissile concentration in metal plates, MOX fuel rods, and a PWR 17x17 fresh fuel assembly [5]. The work described in this paper is focused on investigating the use of SINRD to measure the $^{235}$U and $^{239}$Pu content in PWR 17x17 spent LEU and spent MOX fuel assemblies via Monte Carlo N-Particle eXtended transport code (MCNPX) [6] simulations. The results from these simulations were used to optimize the detector configuration, assess the sensitivity and penetrability of SINRD to partial defects (i.e. missing fuel pins) and obtain a better understanding of the underlying physics of this measurement technique.

We varied the fuel burnup from 10-GWd to 50-GWd (in 10-GWd increments) to observe how the measured response changes as a function of $^{235}$U and $^{239}$Pu content in the fuel. SCALE 5.1 [7] was used to calculate the isotopic composition of PWR spent LEU and MOX fuel at each burnup step. It is important to note that in the MCNPX simulations, the spent fuel isotopics were assumed to be homogeneously distributed in the fuel pins. To assess the sensitivity and penetrability of the SINRD technique, we uniformly removed fuel pins from three different regions of the assembly assuming four-quadrant symmetry and replaced them with depleted uranium (DU) pins. The goal of this analysis is to calculate the percent change in the SINRD ratios per pin removed for each region to determine the minimum number of diverted rods that can be detected with a 2σ confidence level.

## 2. Description of Measurement System

PWR 17x17 spent LEU and MOX fuel assemblies were simulated in water (with and without 2200-ppm of boron) to determine how the scattering of neutrons in water affects the detector response. Spontaneous fission neutrons from $^{244}$Cm were used to self-interrogate the spent fuel pins in the MCNPX simulations of SINRD. The concentration of $^{235}$U and $^{239}$Pu in the spent fuel pins was determined by measuring the distinctive resonance absorption lines from $^{235}$U and $^{239}$Pu using both $^{235}$U and $^{239}$Pu fission chambers (FC) placed adjacent to the side of the fuel assembly. Ratios of different fission chambers were used to reduce the sensitivity of the measurements to extraneous material present in fuel (e.g. fission products). This also reduces the number of unknowns we are trying measure because the neutron source strength and the detector-fuel assembly coupling cancels in the ratio. The specifications used to model the fuel assembly are given in Table 1.

| **Specifications** | | **PWR 17x17** |
|---|---|---|
| Assembly width (square) | | 212 mm |
| Lattice dimensions | | 17 x 17 |
| Number of pins per assembly | | 264 |
| Fuel material | | $UO_2$ / MOX |
| Initial Fissile Content | LEU Fuel | 4.0 at% $^{235}$U |
| | MOX Fuel | 4.0 wt% Pu |
| Cladding material | | Zircaloy 2 |
| Outer fuel diameter | | 9.00 mm |
| Outer clad diameter | | 10.0 mm |
| Fuel element pitch | | 12.5 mm |
| Moderator | | Light Water |

**Table 1:** Characteristics of PWR 17x17 spent fuel assembly.

The SINRD detector unit is located adjacent to the assembly and is approximately 21.3-cm long, 10.4-cm high, and 9.4-cm wide. In order to reduce the background from thermal neutrons, the sides and back of the detector pod were covered with either 1.0-cm of boron carbide ($B_4C$) or 1.0-mm of Cd. The outer $^{235}$U fission chamber (behind $B_4C$) was embedded in polyethylene to thermalize the fast neutrons that penetrated the boron shielding to increase counting statistics. The neutron flux entering the detector pod was measured using two fission chambers. The bare $^{235}$U fission chamber was used to measure the entire neutron spectrum with thermal-neutron domination, and the outer $^{235}$U fission chamber located behind the $B_4C$ shield was used to monitor the fast neutron flux above neutron energies in the resonance region. The SINRD detector configuration was optimized for both PWR spent LEU and MOX fuel cases based on the different concentrations of $^{239}$Pu relative to $^{240}$Pu present in each case over the burnup range of 0 to 50 GWd.

## 3. Analysis of PWR Spent LEU Fuel

### 3.1. Optimization of SINRD Detector Ratios and Absorber Filters

The fission chamber ratios that can be used for SINRD consist of Gd+Hf and Cd covered $^{239}$Pu FCs and two neutron flux monitors, Bare $^{235}$U FC and $B_4C$ $^{235}$U FC (or Fast Flux Monitor). In this study, the sensitivity of the SINRD technique to different combinations of filters and monitors was investigated to determine the optimum configuration that maximized the detector ratio signature. Figure 2 shows the optimized detector configuration used to determine the $^{235}$U and $^{239}$Pu content in a PWR spent LEU fuel assembly and the in-growth of plutonium isotopics in spent LEU fuel as a function of burnup.

The Gd+Hf and Cd covered $^{239}$Pu FCs are used to measure the resonance absorption from $^{239}$Pu in the spent fuel. The transmitted flux through each of these filters relative to the $^{239}$Pu ($n,f$) and $^{240}$Pu ($n,\gamma$) cross-sections, as well as, the results from testing various combinations of these absorber filters to maximize the SINRD detector ratio signature for measuring $^{239}$Pu are shown in Fig. 3. It should be noted that in the following results, we refer to the $B_4C$ $^{235}$U FC as Fast Flux Monitor (or FFM).

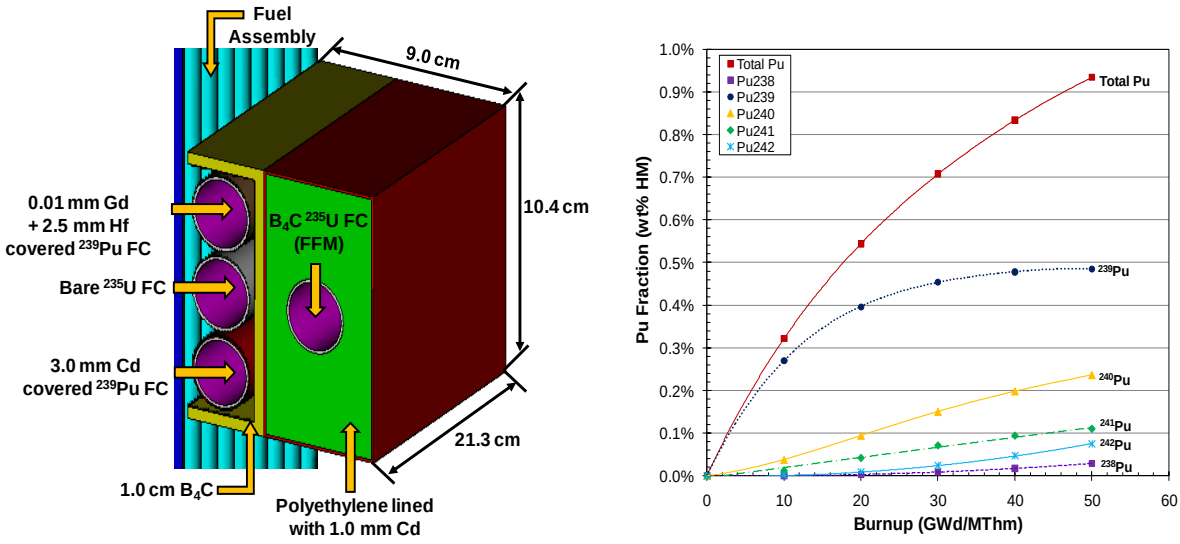


**(a)** SINRD Detector Configuration **(b)** Plutonium Isotopics versus Burnup

**Figure 2.** (a) SINRD detector configuration used to determine $^{235}$U and $^{239}$Pu content in a PWR spent LEU fuel assembly and (b) plutonium isotopics in spent LEU fuel versus burnup.

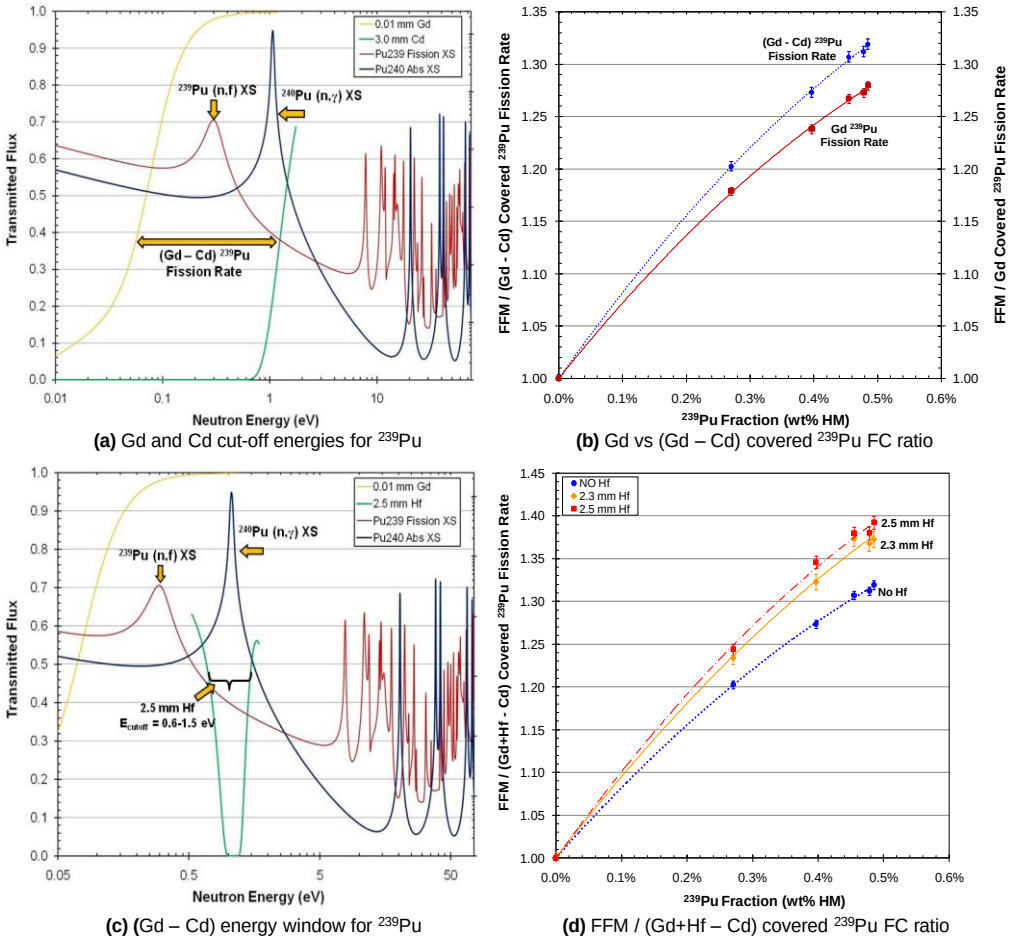


**(a)** Gd and Cd cut-off energies for $^{239}$Pu **(b)** Gd vs (Gd – Cd) covered $^{239}$Pu FC ratio

**(c)** (Gd – Cd) energy window for $^{239}$Pu **(d)** FFM / (Gd+Hf – Cd) covered $^{239}$Pu FC ratio

**Figure 3.** Optimized detector ratios and filters for $^{239}$Pu measurements: (a) the $^{239}$Pu ($n,f$) and $^{240}$Pu ($n,\gamma$) cross-sections within the (Gd – Cd) absorption cut-off energy window, (b) ratio of FFM / Gd covered $^{239}$Pu FC compared to FFM / (Gd – Cd) covered $^{239}$Pu FC ratio versus $^{239}$Pu fraction (wt% HM), (c) transmitted flux through 2.5 mm Hf relative to $^{240}$Pu ($n,\gamma$) cross-section, and (d) the FFM / (Gd – Cd) covered $^{239}$Pu FC ratio versus $^{239}$Pu fraction (wt% HM) for different thicknesses of Hf.

Figure 3a shows how the large $^{239}$Pu resonance at 0.3 eV can be windowed in energy by using the (Gd – Cd) $^{239}$Pu fission rate based on the location of Gd and Cd absorption cut-off energies relative to the $^{239}$Pu fission cross-section. The thick Cd filter (3.0 mm) absorbs the majority of neutrons in the low energy region of the $^{239}$Pu resonance whereas the thin Gd filter (0.01 mm) transmits the majority of these lower energy neutrons. Figure 3b shows the comparison of the FFM / Gd covered $^{239}$Pu FC ratio versus FFM / (Gd – Cd) covered $^{239}$Pu FC ratio as a function of $^{239}$Pu fraction present in the spent fuel. Using the (Gd – Cd) $^{239}$Pu fission rate in the detector ratio, increased the SINRD signature as shown in Fig. 3c. It is also important to note the linearity of the curves shown in Fig. 3b indicates that the SINRD ratio is tracking the $^{239}$Pu concentration in the spent fuel well. The total neutron rate measured in the Fast Flux Monitor (FFM) increases rapidly with the burnup as shown in Fig. 4a. It should be emphasized that the results have been normalized to the fresh fuel case (initial enrichment = 4% $^{235}$U).

To determine if the absorption of low energy neutrons by $^{240}$Pu was decreasing our detector ratio signature, we investigated the effect of adding a Hf filter inside the Gd filter. Figure 3c shows the transmitted flux through a 2.5 mm Hf filter relative to the $^{240}$Pu radiative capture cross-section. The Hf filter absorbs the majority of neutrons in the same energy region as the $^{240}$Pu capture resonance. Figure 3d shows the FFM / (Gd+Hf – Cd) covered $^{239}$Pu FC ratio as a function of $^{239}$Pu fraction present in the spent fuel for no Hf, 2.3 mm and 2.5 mm of Hf. The addition of 2.5 mm Hf to the Gd covered $^{239}$Pu FC increased the SINRD signature by 5.6%.

## 3.2. Verification of Burnup

Next, we investigated the use of our SINRD detector ratios to verify the burnup of a PWR spent LEU fuel assembly. The $^{235}$U and $^{244}$Cm fraction (wt%HM) versus burnup is shown in Fig. 4a. In Fig. 4b and 4c, we show the normalized FFM fission rate and Gd covered $^{239}$Pu to Bare $^{235}$U fission rate ratio as a function of burnup for two possible diversion scenarios where the burnup is misdeclared low and misdeclared high, respectively.

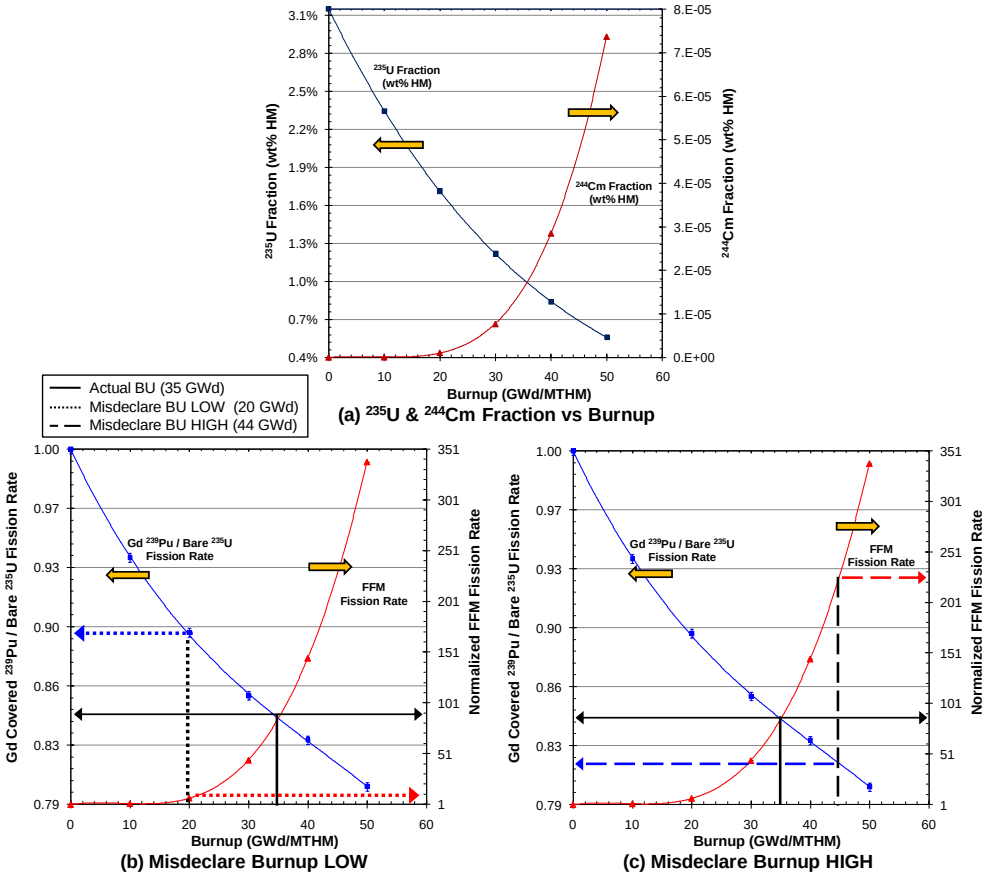


**Figure 4.** Comparison of (a) the $^{235}$U and $^{244}$Cm fraction (wt%HM) versus burnup to (b) and (c) which show the normalized FFM ratio and Gd covered $^{239}$Pu FC / Bare $^{235}$U FC ratio versus burnup for possible diversion scenarios where burnup is misdeclared low and misdeclared high, respectively.

Comparison of Fig. 4a to Fig. 4b and 4c, clearly shows that the normalized fission rate in our FFM is accurately measuring the $^{244}$Cm fraction and that the Gd covered $^{239}$Pu to Bare $^{235}$U fission rate ratio is accurately measuring the $^{235}$U fraction over the burnup range of 0 – 50 GWd. The fact that $^{235}$U fraction decreases as a function of burnup, whereas the $^{244}$Cm fraction increases enables us to verify the burnup of the PWR spent LEU assembly because the proliferator can only get one of these curves right. For instance in Fig. 4b, we show the case where the burnup is misdeclared low. The solid black line indicates the actual burnup of the assembly which is 35 GWd and the solid black arrows point to the expected measured values at this burnup. The misdeclared burnup (20 GWd) is shown by the black dotted line and the dotted red and blue lines correspond to the expected measured values at the lower burnup. It should be noted that when the burnup is misdeclared the expected measured values move in opposite directions. Thus, comparing a set of measurements where the burnup is misdeclared to a reference measurement where the burnup is known would clearly indicate an anomaly in the declaration.

It should also be emphasized that the $^{244}$Cm neutron emission rate from a PWR 17x17 spent LEU fuel assembly is approximately 1.0E+08 n/s and is further amplified by a factor of 2 – 3 by neutron multiplication in the water. This high neutron source term provides adequate counting statistics in the fission chambers to give better than 1% precision in a few minutes for the ratios.

## 4. Analysis of PWR Spent MOX Fuel Assembly

### 4.1. Optimization of SINRD Detector Ratios

In order to better understand the physics of the SINRD technique, we have also simulated the use of SINRD to measure $^{239}$Pu content in a PWR spent MOX fuel assembly. We believe that SINRD technique will work better for a PWR assembly with spent MOX fuel because the $^{239}$Pu concentration is significantly larger and the $^{235}$U concentration is significantly smaller (< 0.15 wt%HM) compared to PWR spent LEU fuel. Figure 5 shows the optimized detector configuration used to determine the $^{239}$Pu content in a PWR spent MOX fuel assembly and the in-growth of plutonium isotopics in spent MOX fuel as a function of burnup. Since the $^{235}$U fraction is less than 0.15 wt% heavy metal in PWR spent MOX fuel, we did not try to measure it. Once again, we have referred to the $B_4C$ $^{235}$U FC as FFM in the results presented in this section.

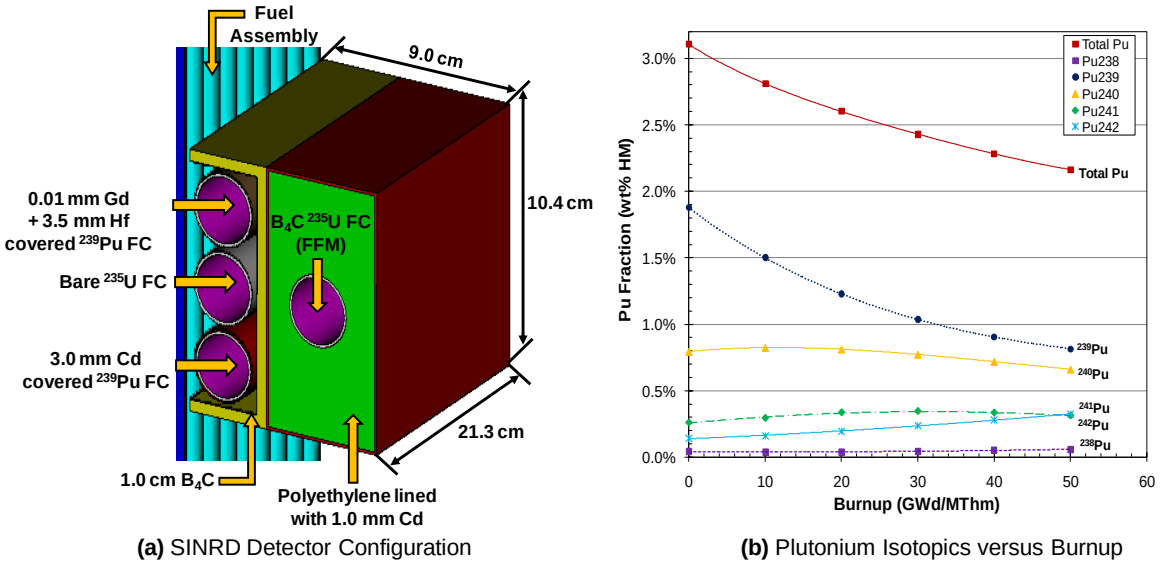


**(a)** SINRD Detector Configuration

**(b)** Plutonium Isotopics versus Burnup

**Figure 5.** (a) SINRD detector configuration used to determine $^{239}$Pu content in a PWR spent MOX fuel assembly and (b) plutonium isotopics in spent MOX fuel versus burnup.

Figure 6 shows the transmitted flux through Gd, Cd, and Hf absorber filters relative to the $^{239}$Pu ($n,f$) and $^{240}$Pu ($n,\gamma$) cross-sections and the results from testing various combinations of these absorber filters to maximize the SINRD detector ratio signature for measuring $^{239}$Pu. It should be emphasized that the results have been normalized to the fresh fuel case (initial enrichment of MOX fuel = 4% Pu).

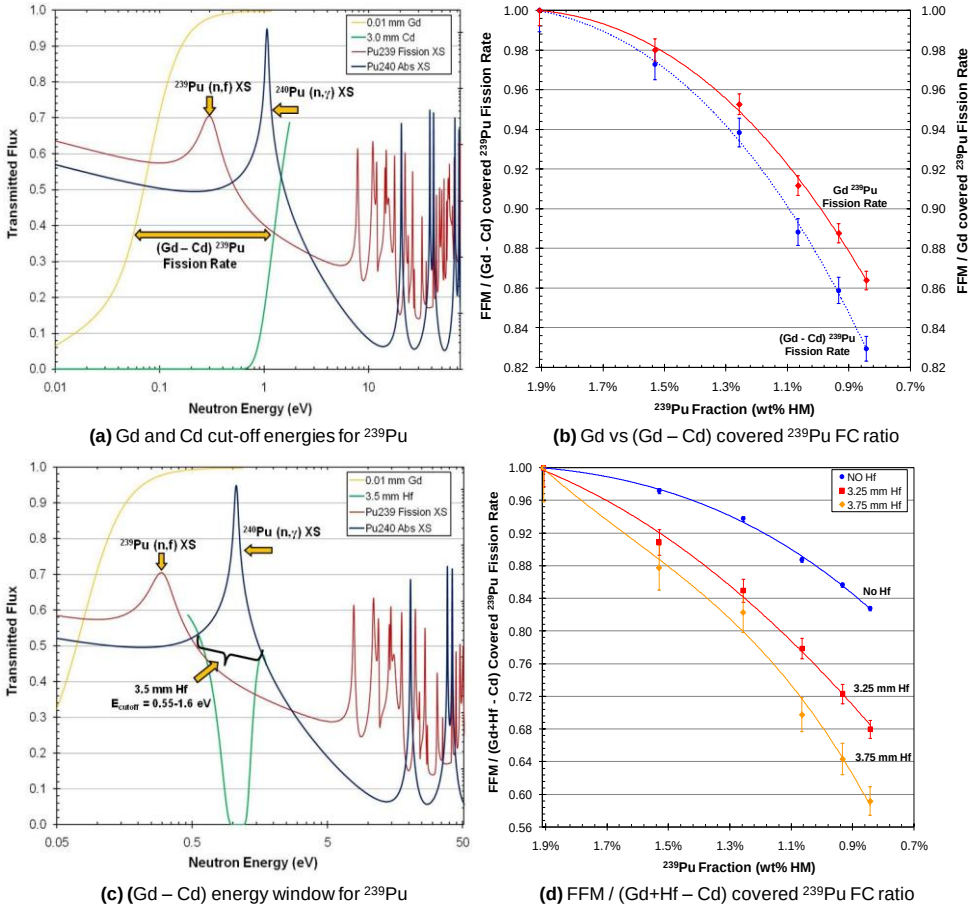


**(a)** Gd and Cd cut-off energies for $^{239}$Pu

**(b)** Gd vs (Gd – Cd) covered $^{239}$Pu FC ratio

**(c)** (Gd – Cd) energy window for $^{239}$Pu

**(d)** FFM / (Gd+Hf – Cd) covered $^{239}$Pu FC ratio

**Figure 6.** Optimized detector ratios and filters for $^{239}$Pu measurements: (a) the $^{239}$Pu (*n,f*) and $^{240}$Pu (*n,γ*) cross-sections within the (Gd – Cd) absorption cut-off energy window, (b) ratio of FFM to Gd covered $^{239}$Pu FC compared to FFM to (Gd – Cd) covered $^{239}$Pu FC ratio versus $^{239}$Pu fraction (wt% HM), (c) transmitted flux through 3.5 mm Hf relative to $^{240}$Pu (*n,γ*) cross-section, and (d) the FFM / (Gd – Cd) covered $^{239}$Pu FC ratio versus $^{239}$Pu fraction (wt% HM) for different thicknesses of Hf.

Similar to Fig. 3a for PWR spent LEU fuel, we show how the large $^{239}$Pu resonance at 0.3 eV can be windowed in energy by using the (Gd – Cd) $^{239}$Pu fission rate in Fig. 6a. Figure 6b shows the ratio of the FFM / Gd covered $^{239}$Pu FC ratio compared to the FFM to (Gd – Cd) covered $^{239}$Pu FC ratio as a function of $^{239}$Pu fraction present in the spent MOX fuel. Using the (Gd – Cd) $^{239}$Pu fission rate in the detector ratio increased the SINRD signature by 4%.

Based on the fact that the $^{240}$Pu concentration is much larger in PWR spent MOX fuel compared to PWR spent LEU fuel, we hypothesized that decrease in our detector ratio signature from the parasitic absorption of low energy neutrons by $^{240}$Pu would be larger for spent MOX fuel. Thus, in order to offset this effect, we would have to increase the thickness of Hf. Figure 6c shows the transmitted flux through a 3.5 mm Hf filter relative to the $^{240}$Pu radiative capture cross-section. Figure 6d shows the FFM / (Gd+Hf – Cd) covered $^{239}$Pu FC ratio as a function of $^{239}$Pu fraction present in the spent fuel for no Hf, 3.25 mm and 3.75 mm of Hf. The addition of 3.75 mm Hf to the Gd covered $^{239}$Pu FC increased the SINRD signature by 32%. It should also be noted that the curves shown in Fig. 6d become more linear as the thickness of Hf is increased. This is important because it indicates that addition of Hf to our SINRD ratio enables us to more accurately track the $^{239}$Pu concentration in the spent MOX fuel.

## 4.2. Verification of Burnup

Next, we investigated the use of SINRD to verify the burnup of a PWR spent MOX fuel assembly. The $^{239}$Pu and $^{244}$Cm fraction (wt%HM) versus burnup is shown in Fig. 7a. In Fig. 7b and 7c, we show the normalized FFM fission rate and the FFM / (Gd+Hf – Cd) covered $^{239}$Pu fission rate ratio as a function of burnup for two possible diversion scenarios where the burnup is misdeclared low and misdeclared high, respectively.

Comparison of Fig. 7a to Fig. 7b and 7c, clearly shows that the normalized FFM fission rate is accurately measuring the $^{244}$Cm fraction and that the FFM to (Gd+Hf – Cd) covered $^{239}$Pu fission rate ratio is accurately measuring the $^{239}$Pu fraction over the burnup range of 0 – 50 GWd. Similar to PWR spent LEU case, our ability to verify the burnup of the assembly is based on the fact that $^{239}$Pu fraction decreases, whereas the $^{244}$Cm fraction increases as a function of burnup. Thus, a proliferator who misdeclared the burnup of the assembly could only get one of these curves right because the expected measured values move in opposite directions.

In a PWR 17x17 spent MOX fuel assembly, the $^{244}$Cm neutron emission rate is approximately 5.0E+08 n/s (~5x greater than a PWR spent LEU fuel assembly) and is further amplified by a factor of 2 – 3 by neutron multiplication in the water. This higher neutron source term in spent MOX fuel enables adequate counting statistics in the fission chambers to better than 1% precision for the ratios to be achieved in less than half the time that is required for spent LEU fuel.

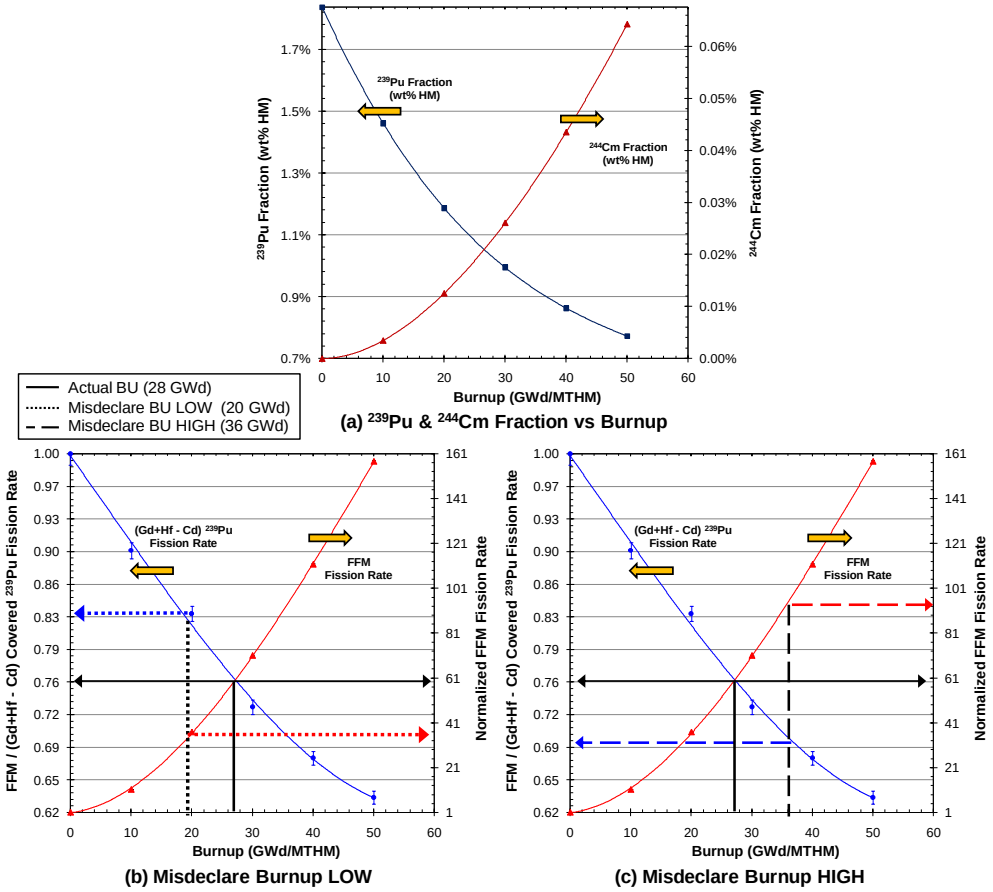


**Figure 7.** Comparison of (a) the $^{239}$Pu and $^{244}$Cm fraction (wt%HM) versus burnup to (b) and (c) which show the normalized FFM ratio and FFM / (Gd+Hf – Cd) covered $^{239}$Pu FC ratio versus burnup for diversion scenarios where burnup is misdeclared low and misdeclared high, respectively.

## 5. Sensitivity of SINRD to Partial Defects

In general, there are two different models for the diversion of fissile material from a fuel assembly. The first is to misdeclare the burnup of the assembly, and the second is to remove fuel pins and to replace them with depleted uranium or iron pins. In the first model, the fissile material distribution is the same as for the calibration standard; however, for the second diversion model, the location of the pin diversion will affect the measured response based on the penetrability of the measurement technique.

Since the fission detector package can be applied to any of the four sides of the assembly, four-quadrant symmetry was assumed in the fuel loading and fuel removal. The penetrability of the SINRD technique was assessed by uniformly removing fuel pins from three different regions of the assembly

where Region 1 consists of two rows on the outer surface of the assembly, Region 2 consists of rows in the mid region, and Region 3 consists of rows in the center of the assembly. The pin removal locations of defects for Regions 1 - 3 in PWR 17x17 fuel assembly is shown in Fig. 8.

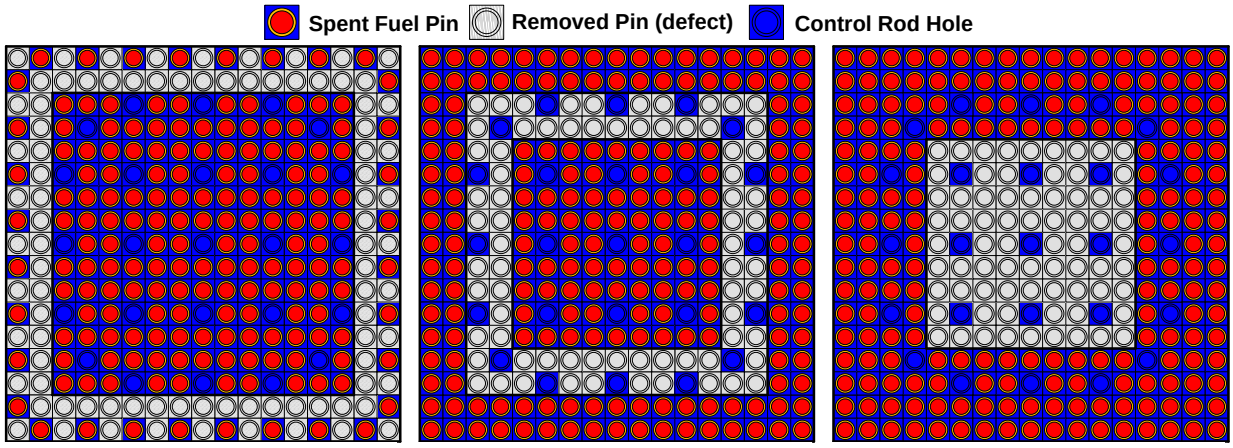


**Figure 8.** Pin removal locations of defects for Regions 1 (a), 2 (b) and 3 (c) in PWR 17x17 fuel assembly where the white pin locations represent the pins that were removed, and the blue locations are the control rods.

In Table 2, the sensitivity of six different SINRD detector ratios with 6.25%, 15%, and 27% of the total number of pins in the PWR spent fuel assembly removed from Regions 1, 2, and 3 for both spent LEU and spent MOX fuel (burnup = 40 GWd) is given.

| Pin Defects (%) | Detector Ratio (NO boron) | Region 1 (1.25 cm) % Change in Ratio | | Region 2 (3.75 cm) % Change in Ratio | | Region 3 (7.75 cm) % Change in Ratio | |
|---|---|---|---|---|---|---|---|
| | | LEU Fuel | MOX Fuel | LEU Fuel | MOX Fuel | LEU Fuel | MOX Fuel |
| 6.25% Pin Defects | FFM / Bare $^{235}$U | **8.31%** | **9.26%** | **3.67%** | **3.66%** | -1.30% | -1.15% |
| | FFM / Gd-Cd) $^{239}$Pu | 7.39% | 8.91% | 2.15% | 2.63% | **-2.07%** | **-1.70%** |
| | FFM / Gd $^{239}$Pu | 6.77% | 8.01% | 1.82% | 2.12% | -1.92% | -1.55% |
| | FFM / Cd $^{239}$Pu | 2.30% | 2.45% | **0.02%** | **-0.03%** | -1.18% | -0.98% |
| | Bare $^{235}$U/Gd $^{239}$Pu | -2.76% | -2.47% | -2.20% | -1.82% | -0.59% | -0.38% |
| | Bare $^{235}$U/Cd $^{239}$Pu | **-10.8%** | **-13.5%** | **-4.34%** | **-4.38%** | **0.11%** | **0.15%** |
| 15% Pin Defects | FFM / Bare $^{235}$U | **19.9%** | **22.2%** | **8.80%** | **8.78%** | -3.12% | -2.75% |
| | FFM / Gd-Cd) $^{239}$Pu | 17.7% | 21.4% | 5.16% | 6.32% | **-4.98%** | **-4.09%** |
| | FFM / Gd $^{239}$Pu | 16.2% | 19.2% | 4.37% | 5.10% | -4.61% | -3.71% |
| | FFM / Cd $^{239}$Pu | 5.51% | 5.87% | **0.06%** | **-0.06%** | -2.83% | -2.36% |
| | Bare $^{235}$U/Gd $^{239}$Pu | -6.63% | -5.93% | -5.27% | -4.38% | -1.41% | -0.92% |
| | Bare $^{235}$U/Cd $^{239}$Pu | **-25.9%** | **-32.3%** | **-10.4%** | **-10.5%** | **0.27%** | **0.37%** |
| 27% Pin Defects | FFM / Bare $^{235}$U | **36.3%** | **40.4%** | **16.0%** | **16.0%** | -5.68% | -5.00% |
| | FFM / Gd-Cd) $^{239}$Pu | 32.3% | 38.9% | 9.39% | 11.5% | **-9.06%** | **-7.44%** |
| | FFM / Gd $^{239}$Pu | 29.6% | 35.0% | 7.95% | 9.27% | -8.38% | -6.76% |
| | FFM / Cd $^{239}$Pu | 10.0% | 10.7% | **0.11%** | **-0.11%** | -5.16% | -4.30% |
| | Bare $^{235}$U/Gd $^{239}$Pu | -12.1% | -10.8% | -9.60% | -7.97% | -2.56% | -1.67% |
| | Bare $^{235}$U/Cd $^{239}$Pu | **-47.1%** | **-58.8%** | **-18.9%** | **-19.1%** | **0.49%** | **0.67%** |

**Table 2:** Sensitivity of six different SINRD detector ratios with 6.25%, 15%, and 27% partial defects removed from Regions 1, 2, and 3 for both spent LEU and spent MOX fuel (burnup = 40 GWd).

The highlighted values shown in Table 2 correspond to the MAXIMUM positive and negative percent change in ratios for **6.25%**, **15%**, **27%** partial defects removed from each region. To help distinguish the different fuel types, slightly darker shades of these colors were used for PWR spent MOX fuel. For

PWR spent LEU fuel, a count time of 500 seconds was used, whereas, a count time of 250 seconds was used for PWR spent MOX fuel. These different count times reflect the different concentrations of $^{244}$Cm in spent LEU fuel versus spent MOX fuel. It is also important to emphasize that the percent change in detector ratio was greater than 2σ uncertainty for ALL ratios in ALL regions except for the Bare $^{235}$U FC to Cd covered $^{239}$Pu FC ratio for PWR spent LEU in Region 3 (cell has been shaded gray).

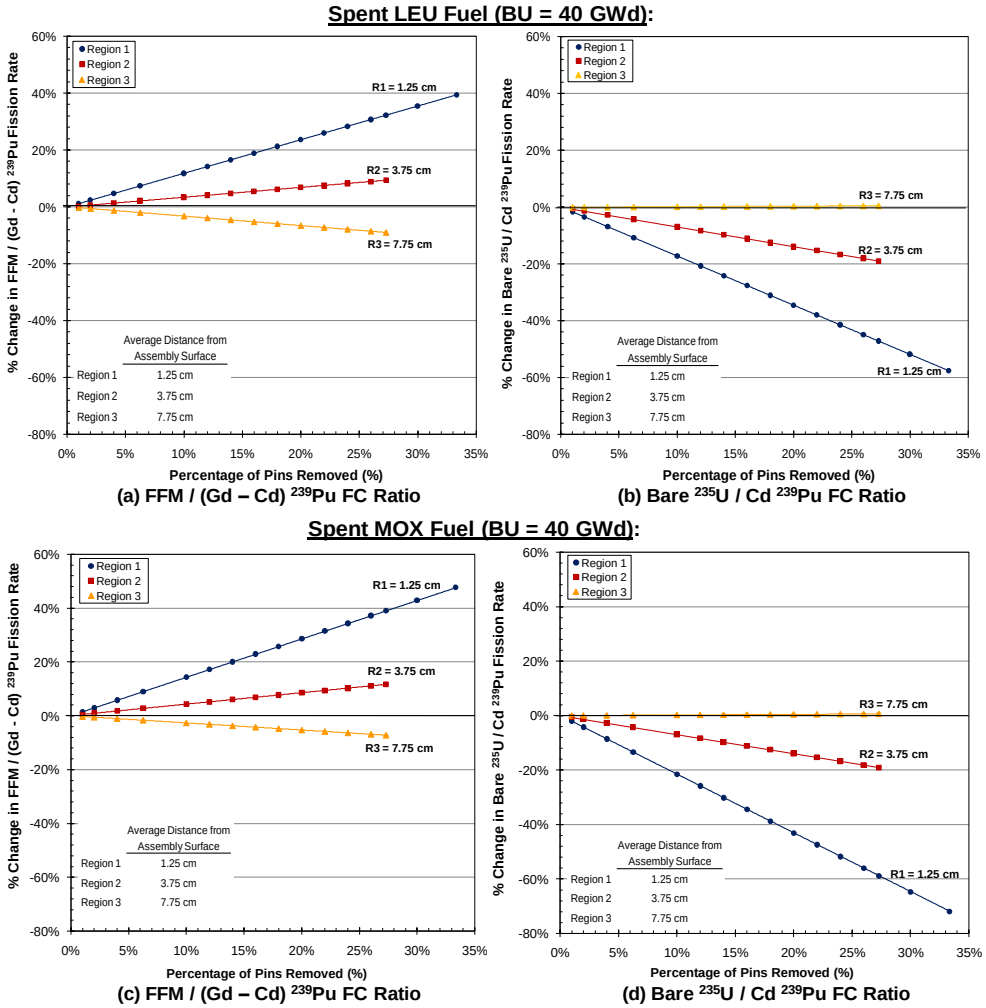


**Figure 9.** Sensitivity to partial defects: (a) and (c) % change in FFM / (Gd-Cd) covered $^{239}$Pu fission rate ratio versus percentage of pins removed for *Spent LEU Fuel* and *Spent MOX Fuel*, respectively (BU = 40 GWd), (b) and (d) % change in Bare $^{235}$U / Cd covered $^{239}$Pu fission rate ratio versus percentage of pins removed for *Spent LEU Fuel* and *Spent MOX Fuel*, respectively (BU = 40 GWd).

The sensitivity of two different SINRD detector ratios to partial defects for PWR spent LEU fuel and spent MOX fuel at a burnup of 40 GWd is shown in Fig. 9. Figures 9a and 9c show the percent change in FFM / (Gd-Cd) covered $^{239}$Pu fission rate ratio as a function of percentage of pins removed for *Spent LEU Fuel* and *Spent MOX Fuel*, respectively. In both cases, the sensitivity to partial defects is highest in Region 1 (two rows on the outer surface of the assembly). Based on these results (9a and 9c), it should be noted that there exists a combination of pins from Region 2 and Region 3 that could result in 0% percent change in FFM / (Gd-Cd) covered $^{239}$Pu FC ratio.

Figures 9b and 9d show the percent change in the Bare $^{235}$U / Cd covered $^{239}$Pu fission rate ratio versus percentage of pins removed for *Spent LEU Fuel* and *Spent MOX Fuel*, respectively. Similar to the results shown in Fig. 9a and 9c, the sensitivity to partial defects is highest in Region 1 for both cases; however, the results shown in 9b and 9d go in the opposite direction as the results shown in 9a and 9c. Thus, the percent change in the Bare $^{235}$U / Cd covered $^{239}$Pu fission rate ratio could be used in conjunction with the percent change in FFM / (Gd-Cd) covered $^{239}$Pu fission rate ratio such that

there is no combination of pins from Regions 2 and 3 that could result in a 0% percent change in the detector ratio.

For each case, error propagations (see Apendix A) were used to calculate the resulting uncertainties in the percent change in the ratio of the FFM / (Gd – Cd) covered $^{239}$Pu FC and in the percent change in the ratio of the Bare $^{235}$U FC / Cd covered $^{239}$Pu FC. The uncertainties in these ratios were between 0.5% – 0.8% for count times of 500 seconds and 250 seconds for PWR spent LEU fuel and spent MOX fuel, respectively. Thus, this type measurement could show the departure from a reference fuel assembly with no defects. It should be emphasized that in all fuel assembly measurements, a reference assembly for calibration is assumed.

## 6. Conclusions

We have simulated the change in different SINRD detector ratios over a burnup range of 0 – 50 GWd using MCNPX. Most of the SINRD FC ratios have the Fast Flux Monitor rate (FFM) in the numerator where the FFM (or $B_4C$ $^{235}$U FC) is simply a fast-neutron flux monitor that measures the neutron source emission rate. The FFM / (Gd+Hf – Cd) covered $^{239}$Pu fission rate ratio is sensitive to the $^{239}$Pu content in both PWR spent LEU fuel and spent MOX fuel assemblies. The SINRD signature for $^{239}$Pu concentration has not saturated for the $^{239}$Pu fraction present in both cases over the burnup range of 0 to 50 GWd; however, the $^{239}$Pu concentration in a PWR spent LEU fuel assembly is approaching saturation at a burnup of 50 GWd. For a factor of two change in the $^{239}$Pu concentration, the signature ratio changes by 21% in water. Therefore, the sensitivity of the method to partial defects is limited to significant (> 10%) changes in the $^{239}$Pu linear loading. This densitometry method requires a calibration with a reference assembly of similar geometry. However, the SINRD method uses the ratio of the FC detectors, so most of the systematic errors related to calibration and positioning cancel in the ratios.

The purpose of this paper was to study the SINRD method for PWR 17x17 spent LEU and spent MOX fuel assemblies. For the cases simulated in this paper, the spent fuel pins in the assembly present an approximate uniform sample to the transmitted neutrons because the self-shielding is small for individual pins and the Pu concentration was assumed to be homogeneously distributed in the pins. For spent fuel assemblies, the initial $^{235}$U enrichment (LEU fuel) or initial Pu loading (MOX fuel) is tailored for the pin positions so that the in-growth of Pu (and burnup) is similar for the different pin positions. For the normal application of neutron (or gamma-ray) densitometry techniques, the sample is assumed to be homogeneous so that the transmitted beam provides the average concentration of the isotope of interest. This homogeneity is the normal condition for solutions and bulk powder, but not for fuel assemblies.

Future work will look at using SINRD to measure the fissile content in LWR spent fuel assemblies without the use of the Pu fission chambers. By using $^{235}$U fission chambers plus metal foils to filter the neutron energy, we can still focus the measurement on the low-energy Pu resonances. The ratio of $^{235}$U fission chambers with selected foil filters provide neutron energy spectral information that can be used to “fingerprint” the actinide loadings in spent fuel assemblies. In addition, the measurement of the $^{235}$U and the $^{244}$Cm can verify the burnup so that the burnup codes can provide the Pu isotopic ratios.

## 7. Acknowledgements

We would like to acknowledge the Program of Technical Assistance to the IAEA (POTAS) and the Department of Energy National Nuclear Security Administration’s Office of Global Security Engagement and Cooperation (NA-242) for their support in the development of the SINRD method. The IAEA has provided useful guidance and support for the activity.

## 8. References

[1] A.M. LaFleur, W.S. Charlton, H.O. Menlove, M.T. Swinhoe, *"Nondestructive Measurements of Fissile Material Using Self-Indication Neutron Resonance Absorption Densitometry (SINRAD),"* Proceedings of 8th International Conference on Facility Operations – Safeguards Interface, Portland, OR, March 30 – April 4, 2008.

[2] H.O. Menlove, C.D. Tesche, M.M. Thorpe, R.B. Walton, *"A Resonance Self-Indication Technique for Isotopic Assay of Fissile Materials,"* Nucl. Appl., **6**, 401 (1969).

[3] *"Nondestructive Assay of SEFOR Fuel Rods,"* Los Alamos National Laboratory Program Status Report April-June 1969, LA-4227-MS (1969).

[4] *"Neutron Self-Indication Assay of SEFOR Fuel Rods,"* Los Alamos National Laboratory Program Status Report July-September1969, LA-4315-MS (1969).

[5] A.M. LaFleur, W.S. Charlton, H.O. Menlove, M.T. Swinhoe, "Use of Self-Interrogation Neutron Resonance Densitometry (SINRD) to Measure the Fissile Content in Nuclear Fuel," Proceedings of 49th Annual INMM Meeting, Nashville, TN, July 13 – 17, 2008.

[6] D. B. Pelowitz ed., *"MCNPX User's Manual, Version 2.5.0,"* Los Alamos National Laboratory Report, LA-CP-05-0369 (2005).

[7] *SCALE: A Modular Code System for Performing Standardized Computer Analyses for Licensing Evaluations,* ORNL/TM-2005/39, Version 5.1, Vols. I-III, November 2006. Available from Radiation Safety Information Computational Center at Oak Ridge National Laboratory as CCC-732.

# APPENDIX A

Count Rate in Detector

The count rate in detector (*i*) was calculated using the following equation where the subscript *i = $B_4C$ $^{235}U$, Bare $^{235}U$, Gd+Hf covered,* or *Cd covered $^{239}Pu$ fission chambers* corresponding to the particular detector on which fission rate was tallied in MCNPX. The superscript *k = $^{238}U$ or $^{240}Pu$* corresponding to the spontaneous fission source in fresh LEU fuel or fresh MOX fuel, respectively.

$$CR_i = m_{SF}^k \cdot y_{SF}^k \cdot MCNPX\ \ Tally_i \tag{A.1}$$

where

$m_{SF}^k\ \left[g\right] \equiv$ Mass of the self-interrogating spontaneous fission source (*k*) in fuel

$y_{SF}^k\ \left[n/s \cdot g\right] \equiv$ Spontaneous fission yield of the self-interrogating spontaneous source (*k*) in fuel

$MCNPX\ \ Tally_i\ \left[fissions/source\ neutron\right] \equiv$ Fission rate tally in detector (*i*) from MCNPX output

Assuming a count time, $t_C$, the total number of counts in detector (*i*) and the corresponding standard deviation the counts were calculated using the following equations:

$$\begin{aligned} C_i &= CR_i \cdot t_C = m_{SF}^k \cdot y_{SF}^k \cdot MCNPX\ \ Tally_i \cdot t_C \\ \sigma_i &= \sqrt{C_i} \end{aligned} \tag{A.2}$$

Using the total number of counts calculated for each detector, six different detector ratios and corresponding standard deviations were calculated from the following equations (A.3) – (A.8):

$$1)\ R_1 = \frac{C_{B_4C}}{C_{Bare}},\ \sigma_{R1} = \frac{C_{B_4C}}{C_{Bare}}\sqrt{\left(\frac{\sigma_{B_4C}}{C_{B_4C}}\right)^2 + \left(\frac{\sigma_{Bare}}{C_{Bare}}\right)^2} \tag{A.3}$$

$$2)\ R_2 = \frac{C_{B_4C}}{C_{Gd-Cd}},\ \sigma_{R2} = \frac{C_{B_4C}}{C_{Gd-Cd}}\sqrt{\left(\frac{\sigma_{B_4C}}{C_{B_4C}}\right)^2 + \left(\frac{\sigma_{Gd-Cd}}{C_{Gd-Cd}}\right)^2} \tag{A.4}$$

$$3)\ R_3 = \frac{C_{B_4C}}{C_{Gd}},\ \sigma_{R3} = \frac{C_{B_4C}}{C_{Gd}}\sqrt{\left(\frac{\sigma_{B_4C}}{C_{B_4C}}\right)^2 + \left(\frac{\sigma_{Gd}}{C_{Gd}}\right)^2} \tag{A.5}$$

$$4)\ R_4 = \frac{C_{B_4C}}{C_{Cd}},\ \sigma_{R4} = \frac{C_{B_4C}}{C_{Cd}}\sqrt{\left(\frac{\sigma_{B_4C}}{C_{B_4C}}\right)^2 + \left(\frac{\sigma_{Cd}}{C_{Cd}}\right)^2} \tag{A.6}$$

$$5)\ R_5 = \frac{C_{Bare}}{C_{Gd}},\ \sigma_{R5} = \frac{C_{Bare}}{C_{Gd}}\sqrt{\left(\frac{\sigma_{Bare}}{C_{Bare}}\right)^2 + \left(\frac{\sigma_{Gd}}{C_{Gd}}\right)^2} \tag{A.7}$$

$$6)\ R_6 = \frac{C_{Bare}}{C_{Cd}},\ \sigma_{R6} = \frac{C_{Bare}}{C_{Cd}}\sqrt{\left(\frac{\sigma_{Bare}}{C_{Bare}}\right)^2 + \left(\frac{\sigma_{Cd}}{C_{Cd}}\right)^2} \tag{A.8}$$

Sensitivity to Partial Defects

Next, fuel rods were uniformly removed from Regions (1), (2) and (3) of the assembly and the six detector ratios given above were recalculated. The perturbed detector ratio, *D*, resulting from the uniform removal of fuel rods is given in Eq. (A.9):

$$D_x^{(k)} = \frac{C_i^{(k)}}{C_j^{(k)}},\ \sigma_{D(x,k)} = \frac{C_i^{(k)}}{C_j^{(k)}}\sqrt{\left(\frac{\sigma_i^{(k)}}{C_i^{(k)}}\right)^2 + \left(\frac{\sigma_j^{(k)}}{C_j^{(k)}}\right)^2} \tag{A.9}$$

where

*k = 1, 2, 3*, corresponding to the region from which fuel rods were removed from the assembly
*x = 1,…, 6*, corresponding to the six detector ratios given in Eq. (A.3) – (A.8)

The subscript *i* corresponds to the detector used in the *numerator* of the six ratios where *i = $B_4C$ $^{235}U$ or Bare $^{235}U$ fission chambers*. The subscript *j* corresponds to the detector used in the *denominator* of the six ratios where *j = Bare $^{235}U$*, *Gd covered,* or *Cd covered fission chambers*.

To assess the sensitivity of each region in the assembly to the uniform removal of fuel rods, the percent-difference, *P*, between the detector ratio, *R* (*no defects*), and the detector ratio, *D* (*partial defects*), and corresponding standard deviations were calculated for each region (*k*) using the following equations:

$$P_x^{(k)} = \frac{R_x^{(k)} - D_x^{(k)}}{R_x^{(k)}} \times 100$$

$$let\ A = R_x^{(k)} - D_x^{(k)}\ and\ \sigma_A = \sqrt{\left(\sigma_{R(x,k)}\right)^2 + \left(\sigma_{D(x,k)}\right)^2} \tag{A.10}$$

$$\Rightarrow \sigma_{P(x,k)} = \frac{A_x^{(k)}}{R_x^{(k)}}\sqrt{\left(\frac{\sigma_{A(x,k)}}{A_x^{(k)}}\right)^2 + \left(\frac{\sigma_{R(x,k)}}{R_x^{(k)}}\right)^2}$$